As originally published in the SMTA Proceedings.

# Kinetics of the Accumulation of a Layer of Bismuth at the Anode of a Sn-Bi Based Solder Joint During Current Stressing

Javier Flores, Faramarz Hadian, Sitaram Panta, Eric Cotts, Ph.D.
Binghamton University
ecotts@binghamton.edu

**Abstract**
Measurements of the electrical resistance of low temperature solder, SnBi microelectronic interconnects, during current stressing were shown to provide sensitive indicators of the thickness of continuous layers of Bi accumulated at the anode. A linear rate of Bi accumulation at the anode of a SnBi based solder joint (for a constant temperature and current density) was observed. A Black's equation for failure (based upon a criterion of a set increase in electrical resistance of the solder joint, e.g., twenty percent) yielded good fits over a temperature range extending from 90 to 125°C.

Key words: Low temperature solders, electromigration, failure analysis, Black's equation, reliability, atomic diffusion

## I. Introduction

Interest continues to grow in low temperatures solders, such as near eutectic SnBi, [1]–[13]. Successful implementation of these solders requires careful characterization of their failure rates during current stressing. SnBi solder joints are subjected to current densities of more than 2 kA/cm$^2$, and operating temperatures up to 100°C [3], [14]. Such current stressing can result in the accumulation of Bi at the anode of the solder joint, and corresponding increases in the electrical resistance. An increase of twenty percent of the initial resistance the solder joint constitutes a failure by JEDEC standards [15]. Besides direct alteration of some electrical signals, the formulation of a continuous layer of Bi at the anode of the SnBi solder joint will affect its mechanical response. Thus, we seek a quantitative expression for the rate of accumulation of Bi as a function of current density and temperature, and a corresponding expression for the mean time to failure, of SnBi based solder joints.

## II. Background

Previous work revealed a direct correlation between the change in the electrical resistance of SnBi based solder joints and Bi accumulation at the anode during current stressing [16], [17]. Thus, expressions for the flux of Bi atoms in Sn during current stressing were used to develop quantitative expressions for the change in the electrical resistance of near eutectic SnBi based solder joints as a function of time, temperature and current density. Previous studies found that $J_{EM}$, the electromigration flux of Bi atoms in Sn during current stressing, dominates the total effective flux [18]–[20]. This results in simplification of expressions for $J_{EM}$:

$$J_{EM} = \frac{Ce\rho_{Sn(Bi)}}{k} DZ^* \frac{j}{T}, \qquad (1)$$

where C is Bismuth concentration corresponding to the solubility limit of Bi in Sn at the operating temperature, T, e is the electron charge, $\rho_{Sn(Bi)}$ is the electrical resistivity of Sn containing the equilibrium concentration of Bi, k is the Boltzmann constant, D is the diffusion coefficient of Bi in Sn, $Z^*$ is the effective charge number of Bi during electromigration, and j is the applied current density. With (1) we can obtain an equation for the thickness, y, of the Bi layer at the anodes as a function of time [16]:

$$y = \frac{C(DZ^* e\rho j)V_m}{kTN_A}\left(1 + 0.57\frac{X_{Bi}}{X_{Sn}}\right) t = bt\ , \qquad (2),$$

where $V_m$ is the molar volume of SnBi; and $X_{Bi}$ and $X_{Sn}$ are the mass fractions of Bi and Sn in the SnBi alloy, respectfully. Because the electrical resistivity of Bi, $\rho_{Bi}$, is an order of magnitude larger than the electrical resistivity of SnBi, $\rho_{SnBi}$, an expression for the change in the solder joint electrical resistance, percent increases in resistance, $\Delta R$, to the initial electrical resistance of the solder joint, $R_o$, may be identified:

$$\frac{\Delta R}{R_o} = \frac{y}{h}\left(\frac{\rho_{Bi}}{\rho_{SnBi}} - 1\right), \qquad (3)$$

where y is the Bi layer thickness, h is the joint height, $\rho_{Bi}$ is the electrical resistivity of pure Bi, and $\rho_{SnBi}$ is the electrical resistivity of eutectic SnBi. Substituting (2) in to (3), and defining failure as a 20 percent increase in resistance, an equation for the mean time to failure (MTF) can be derived:

$$MTF = \frac{B}{j} exp\left(\frac{E_D}{kT}\right), \qquad (4)$$

with

$$B = \frac{0.2hN_aT}{\left(\frac{\rho_{Bi}}{\rho_{SnBi}} - 1\right)e\rho_{Sn(Bi)}V_m C D_o Z^*\left(1 + 0.57\frac{X_{Bi}}{X_{Sn}}\right)} \qquad (5)$$

where $E_D$ is the activation energy of Bi diffusion in Sn, $D_o$ is the diffusivity pre-exponential of Bi in Sn, and $N_A$ is Avogadro's number.

A simpler expression (Black's equation [21]) for the MTF may be utilized,

$$MTF = \frac{A'}{j} exp\left(\frac{E_a}{kT}\right), \qquad (6)$$

where $A'$ is a constant and the apparent activation energy, $E_a$, is not equal to $E_D$. Black's equation (6) may often be the most utilitarian approach to fitting and extrapolating current stressing failure data. One may note that the details of (5) may reveal useful relations for practitioners. For instance, (5) indicates that B is proportional to h, i.e. independent of other influences, failure times will significantly less for smaller solder joints. Furthermore, (5) provides clear indication of

expected changes in failures times as the Bi content, $X_{Bi}$, of solder is changed.

Previous work utilized Eq. (6) to fit data for MTF versus temperature, T, and current density, j, where most of the data was at a temperature of 105°C, or above [16]. The present work sought to provide additional data in the range of temperatures found in many devices, e.g. near 90°C. This study seeks to extend the range of data on MTF as a function of j and T to lower temperatures, and provide a Black's equation to characterize *MTF(j,T)*.

### III. Experimental

The test vehicle (Fig. 1) for current stressing experiments was composed of a laminate board and a laminate test component joined via a matrix array of cylindrical, 230 µm-diameter solder joints. Test vehicles were fabricated using Sn57BiSbNi solder paste reflowed with a peak temperature of 190°C with a time above liquidus of approximately 60 seconds.

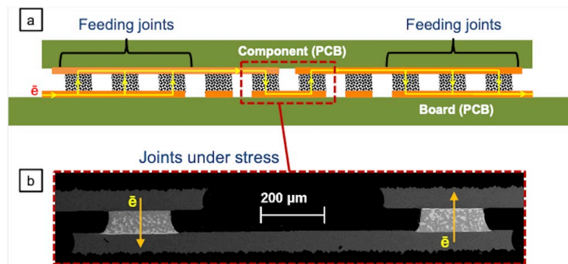


**Figure 1:** a) A schematic drawing of a row of solder joints under current stressing in the test vehicle including feeding joints, jumpers and risk sites. The yellow arow shows the direction of electron flow during electromigration. b) A scanning electron micrograph of an actual cross sectioned risk sites area corresponding to part a. The current was from component to board in one joint, and from board to component in the other joint.

The patterning of the Cu board metallization also allowed simultaneous four-point measurements of the electrical resistance each solder joint, risk site. JEDEC Standard JESD33B (the temperature coefficient of resistance (TCR) method) was utilized to calibrate the resulting electrical resistance versus curves [22] (using a measuring current of 400mA, shown to cause negligible Joule heating). The quantity TCR (which was simply proportional to S):

$$TCR(T_{ref}) = \frac{S}{R(T_{ref})} \quad (7),$$

where $R(T_{ref})$ was the electrical resistance at a value of $T_{ref}$ = 21°C, and quantity, S, was the slope determined from a linear fit to the R versus T data. The mean operating temperature, $T_{mean}$ of a solder joint was then determined for each current density (and a particular ambient temperature, $T_a$) as:

$$T_{mean} = \left(\frac{R(T_{mean})-R(T_a)}{R(T_{ref})*TCR(T_{ref})}\right) + T_a, \quad (8),$$

### IV. Results and Discussion

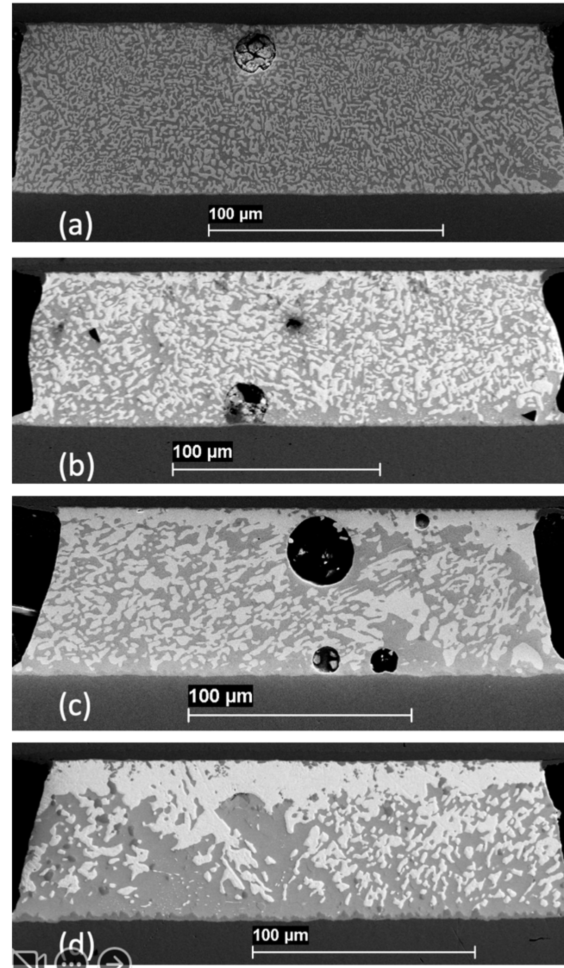


**Figure 2:** Scanning electron microscopy micrographs of samples current-stressed with an applied current density of 5kA/cm$^2$ at 91°C for different amounts of time (a) as-reflowed, i.e. 0, h (b) 375 h, (c) 800 h, (d) 1600 h.

A layer of Bi was observed to accumulate at the anode of these Cu/Sn57BiSbNi/Ni solder joints during current stressing at a constant temperature and current density. For instance, in Fig. 2, scanning electron micrographs of Cu/Sn57BiSbNi/Ni solder joint after current stressing at a current density of 5 kA/cm$^2$ for different periods of time from zero to 1600h, at solder joint temperature of 91°C, are displayed. A continuous layer of Bi is visible at the anode of the sample in Fig. 2(b), and this Bi layer thickens with times, as indicated by the micrographs in Figs. 2 (c) and 2(d). A linear growth rate of Bi at the anode during current stressing at a constant temperature and current density is consistent with equations (1) and (2). This rate of growth depends linearly upon the diffusion constant for Bi in Sn (D in Eq. 2), which is thermally activated, with an activation energy near one electron volt pre atom. That is to say, one would expect that the rate of growth of Bi would depend strongly upon temperature. In fact, Fig. 3 reveals scanning electron micrographs for two different samples, one current stressed

at a temperature of 125°C (Fig. 3(a)) and one current stressed at a temperature of 91°C (Fig. 3(b)) [the current densities were similar for both samples, 4kA/ $cm^2$ for the sample in Fig. 3(a) and 5kA/$cm^2$ for the sample in 3(b), and the current stressing times were the same, 200 h]. The Bi layer which has formed at a temperature of 125°C can be seen to be an order of magnitude thicker than that formed at a temperature 34°C lower (Fig. 3), as would be expected from Eq.2.

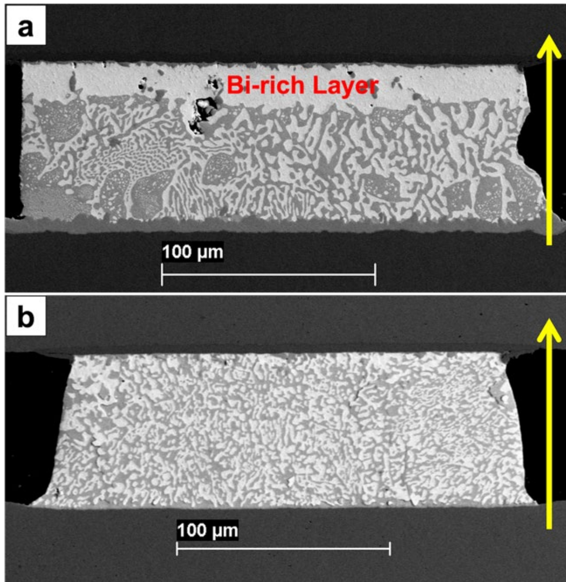


**Figure 3:** Micrographs of samples current-stressed (a) with an applied current density of 4kA/$cm^2$ at 125°C, and (b) with an applied current density of 5kA/$cm^2$ at 91°C. Both were stressed for 200 hours.

Four terminal measurements of the electrical resistance of a large number of Cu/Sn57BiSbNi/Ni solder joints were conducted as a function of time during current stressing at specific combinations of constant temperature and constant current density. For instance, a plot of the percentage change of electric resistance versus time for twenty-nine similarly prepared Cu/Sn57BiSbNi/Ni solder joints under going current stressing at a temperature of 91°C is presented in Fig. 4(a). Examination of these plots of electrical resistance versus time of individual solder joints undergoing current stressing revealed similarly shaped curves, though there was significant variation in the initial slope of the change in electrical resistance versus time (Fig. 4(a)). Although most of the percent change in electrical resistance versus time plots had fairly similar slopes, there were some that significantly deviated from such norms, resulting in early fails. This fact is also reflected in a standard Weibull plot (Fig. 4(b)) for this same data.

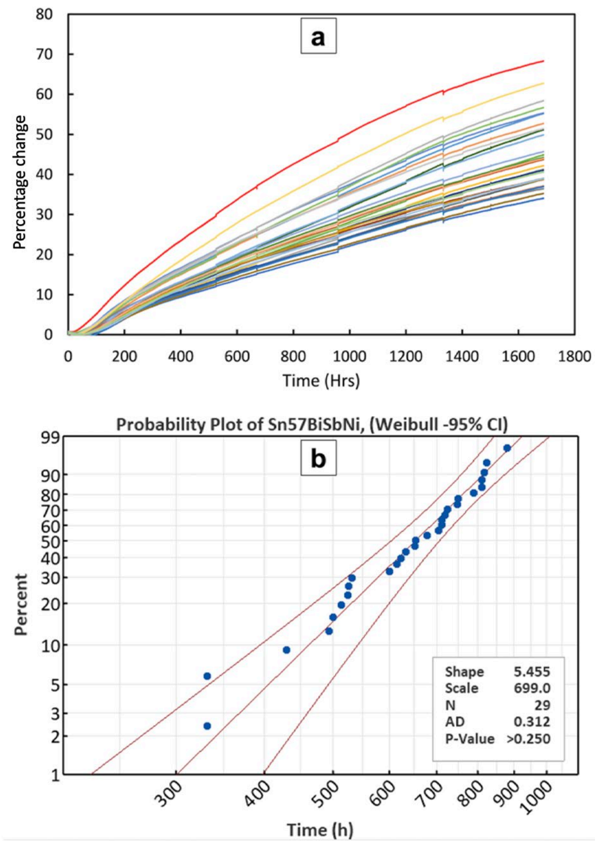


**Figure 4:** (a) Percent change in resistance vs. time curves for 5kA/$cm^2$, 91°C samples. The times to failure for each individual joint were determined by noting when their curves reached 20%. (b) A Weibull plot of the collected failure times.

Additional results of Weibull analysis are presented in Figs. 5 and 6 for specific combinations of current density and temperature for Cu/Sn57BiSbNi/Ni solder joints. The variation in failure distributions upon a change in the temperature of similar samples is presented in Fig. 5. Both of the sample sets analyzed in Fig. 5 were current stressed at 6kA/$cm^2$, while the data was analyzed in two separate groups, corresponding to each sample's temperature (95 or 125°C). The effect of an increase in temperature was clearly discernible on the MTF, as expected in a process dominated by the thermally activated process of atomic diffusion [Eq. 2]. Changing the current density (while holding the temperature constant) during current stressing, also resulted in a change of the MTF (Fig. 6). As expected from a simple Black's equation (Eq. 6) picture, the mean time to failure (MTF) was inversely proportional to the current density.

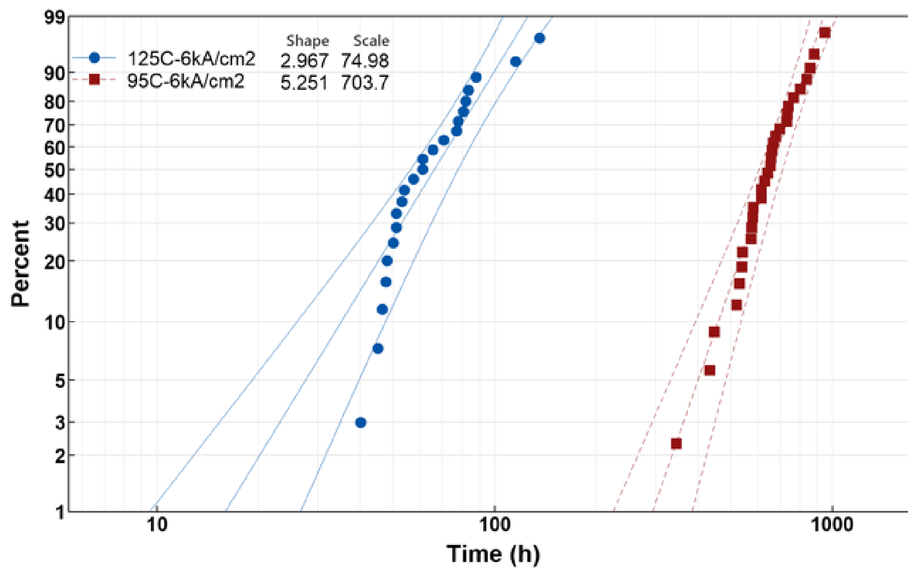


**Figure 5:** Weibull distribution plots (95% confidence interval (CI)) for sample sets current stressed with a current density of 6 kA/cm$^2$ and at one of two different temperatures from 95 and 125$^o$C, as indicated in the figure. The failure criterion was a twenty percent increase in the electrical resistance (four terminal measurement). The data from each sample are displayed in these plots of the percentage of samples failed versus current stressing time, along with the results of the Weibull fitting. The shape and scale for the Weibull fit for each data set are displayed in the legend in the figure.

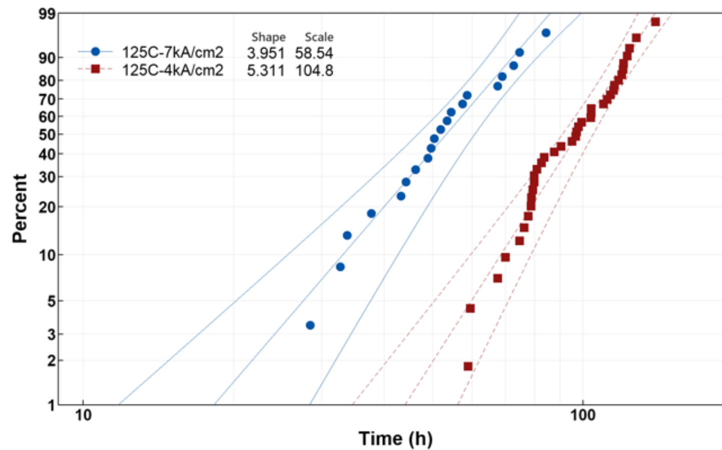


**Figure 6:** Weibull distribution plots (95% CI) for sample sets current stressed at a temperature of 125$^o$C and at one of the current densities from 4 to 7 kA/cm$^2$, as indicated in the figure. The failure criterion was a twenty percent increase in the electrical resistance (four terminal measurement). The data from each sample are displayed in these plots of the percentage of samples failed versus current stressing time, along with the results of the Weibull fitting. The shape and scale for the Weibull fit for each data set are displayed in the legend in the figure.

Analysis of the MTF of near eutectic SnBi based solder joints at different specific values of current density and temperature provides Black's equation for MTF. Plots of the natural logarithm of the mean time to failure (MTF) plus the natural logarithm of the current density versus 1/kT would be expected to be linear, according to Eq. 6 (Black's equation). Such a plot is presented in Fig. 7, along with a linear fit to the data. The activation energy was found to be 0.8 eV. Predictions of failure times at lower temperatures and different current densities may be provided by extrapolation.

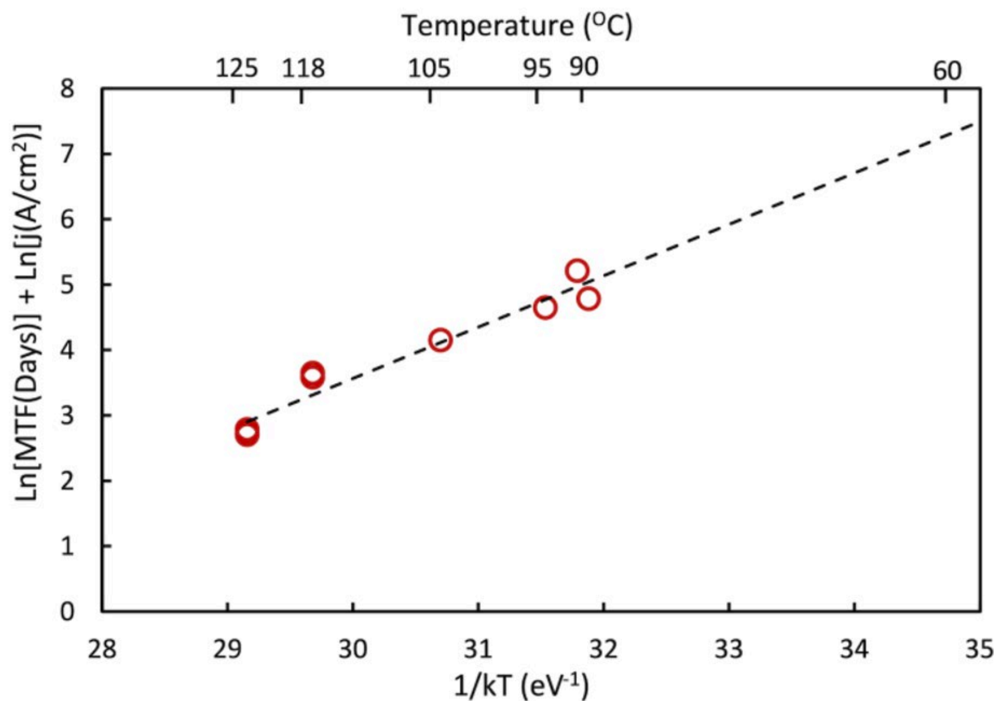


**Figure 7:** A plot of ln(MTF)+ln(j) versus 1/kT for current-stressed Sn57BiSbNi joints under varying current-stressing conditions .

### V. Conclusion

Utilizing the JEDEC current stressing failure criterion that depends upon a twenty percent increase in the electrical resistance of a SnBi based solder joint, and the relation between this change in electrical resistance and the thickness of a Bi layer accumulated at the anode of the solder joint during current stressing, a quantitative expression for MTF as a function of j and T was identified. Fits of this Arrhenius expression yielded a relation between MTF and current density and temperature with an activation energy of 0.8 eV. This single Black's equation was observed to fit observations obtained at operating temperatures, and at significantly higher temperatures. Thus, this formalism provides clear acceleration factors for laboratory current stressing of such low temperature solder joints.

### VI. Acknowledgments

The authors acknowledge Michael Meilunas and Dr. Jim Wilcox of the Universal Instruments Advanced Process Laboratory for their assistance in sample preparation and useful technical discussion. Additional financial support from the IEEC and the Semiconductor Research Corporation (SRC) is also gratefully acknowledged.

### VII. References

[1] F. Wang, L. Liu, D. Li, and M. Wu, "Electromigration behaviors in Sn–58Bi solder joints under different current densities and temperatures," *J. Mater. Sci. Mater. Electron.*, vol. 29, no. 24, pp. 21157–21169, 2018, doi: 10.1007/s10854-018-0264-x.

[2] R. Coyle *et al.*, "Thermal Cycle Reliability of a Low Silver Ball Grid Array Assembled With Tin Bismuth Solder Paste," *Proc. SMTA Int. Rosemont, IL, USA*, pp. 17–21, 2017.

[3] S. P. Lim *et al.*, "Low temperature 1st level interconnect in Packaging and its Challenges," *2021 Int. Conf. Electron. Packag. ICEP 2021*, pp. 49–50, 2021, doi: 10.23919/ICEP51988.2021.9451941.

[4] R. Coyle *et al.*, "The Effect of Peak Reflow Temperature on Thermal Cycling Performance and Failure Mode of Hybrid Low Temperature Solder Joints," in *SMTA International Conference*, 2021, pp. 387–400.

[5] R. Coyle *et al.*, "Interim Thermal Cycling Report on Hybrid , Homogeneous , and Resin Reinforced Low Temperature Solder Joints," in *Proceedings of SMTA International*, 2021, pp. 401–426.

[6] S. Sahasrabudhe *et al.*, "Low Temperature Solder - A Breakthrough Technology for Surface Mounted Devices," in *2018 IEEE 68th Electronic Components and Technology Conference (ECTC)*, May 2018, vol. 2018-May, pp. 1455–1464, doi: 10.1109/ECTC.2018.00222.

[7] L. Wentlent, D. Ph, J. Wilcox, D. Ph, and M. Meilunas, "Thermal Cycling Behaviors of Hybrid

and Homogeneous Low Temperature Solder Interconnects," 2021, pp. 548–554.

[8] F. Wang, H. Chen, Y. Huang, L. Liu, and Z. Zhang, "Recent progress on the development of Sn–Bi based low-temperature Pb-free solders," *J. Mater. Sci. Mater. Electron.*, vol. 30, no. 4, pp. 3222–3243, 2019, doi: 10.1007/s10854-019-00701-w.

[9] J. Zhao, L. Qi, X. M. Wang, and L. Wang, "Influence of Bi on microstructures evolution and mechanical properties in Sn-Ag-Cu lead-free solder," *J. Alloys Compd.*, vol. 375, no. 1–2, pp. 196–201, 2004, doi: 10.1016/j.jallcom.2003.12.005.

[10] L. Zhang, L. Sun, and Y. huan Guo, "Microstructures and properties of Sn58Bi, Sn35Bi0.3Ag, Sn35Bi1.0Ag solder and solder joints," *J. Mater. Sci. Mater. Electron.*, vol. 26, no. 10, pp. 7629–7634, 2015, doi: 10.1007/s10854-015-3400-x.

[11] M. Ribas *et al.*, "Low Temperature Soldering Using Sn-Bi Alloys," in *Proceedings of SMTA International*, 2017, pp. 201–206.

[12] M. Ribas *et al.*, "Development of low-temperature drop shock resistant solder alloys for handheld devices," *Proc. 2013 IEEE 15th Electron. Packag. Technol. Conf. EPTC 2013*, pp. 48–52, 2013, doi: 10.1109/EPTC.2013.6745682.

[13] H. Fu *et al.*, "Process Development of BiSn-based low temperature solder pastes- part- Vi : mechanical shock results on resin reinforced mixed SnAgCu-BiSn solder joints of FCBGA components," in *Proceedings of SMTA International*, 2019, pp. 513–525.

[14] J. Glazer, "Microstructure and mechanical properties of Pb-free solder alloys for low-cost electronic assembly: A review," *J. Electron. Mater.*, vol. 23, no. 8, pp. 693–700, 1994, doi: 10.1007/BF02651361.

[15] "Guideline for Characterizing Solder Bump Electromigration under Constant Current and Temperature Stress," *JEDEC Solid State Technol. Assoc.*, vol. JEP154, 2011.

[16] F. Hadian, J. Flores, and E. Cotts, "The Variation of the Electrical Resistance and Microstructure of SnBi based Solder Joints with Current Stressing," *Jom*, vol. 74, no. 5, pp. 2139–2147, 2022, doi: 10.1007/s11837-022-05255-7.

[17] F. Hadian, S. Panta, J. Flores, and E. J. Cotts, "The Effect of Current Stressing on the Electrical Resistance and Microstructure of Sn-Bi based Solder Joints," in *SMTA International Conference*, 2021, pp. 445–450.

[18] L. T. Chen and C. M. Chen, "Electromigration study in the eutectic SnBi solder joint on the Ni/Au metallization," *J. Mater. Res.*, vol. 21, no. 4, pp. 962–969, 2006, doi: 10.1557/jmr.2006.0113.

[19] X. Gu and Y. C. Chan, "Electromigration in Line-Type Cu/Sn-Bi/Cu Solder Joints," *J. Electron. Mater.*, vol. 37, no. 11, pp. 1721–1726, 2008, doi: 10.1007/s11664-008-0539-8.

[20] W. Zhou, L. Liu, B. Li, and P. Wu, "Fast mass migration in SnBi deposits enhanced by electric current," *Thin Solid Films*, vol. 518, no. 20, pp. 5875–5880, 2010, doi: 10.1016/j.tsf.2010.05.090.

[21] J. R. Black, "Electromigration—A Brief Survey and Some Recent Results," *IEEE Trans. Electron Devices*, vol. 16, no. 4, pp. 338–347, 1969, doi: 10.1109/T-ED.1969.16754.

[22] JEDEC, "Standard Method for Measuring and Using the Temperature Coefficient of Resistance to Determine the Temperature of a Metallization Line," vol. JESD33B, no. October. JEDEC Solid State Technology Association, 2012.